COMMUNICATION

The amphiphilic nanostructure of ionic liquids affects the dehydration of alcohols

Received 00th January 20xx,
Accepted 00th January 20xx

DOI: 10.1039/x0xx00000x

Emma L. Matthewman,[a,b] Bhavana Kapila,[c] Mason L. Grant[a,b] and Cameron C. Weber*[a,b]

The effect of the amphiphilic nanostructure of ionic liquids has been investigated on the dehydration of secondary alcohols to alkenes. The influence of these nanostructures was inverted when an acid catalyst was added to the reaction. This phenomenon was ascribed to a balance between ion-solute interactions and the formation of solute-catalyst hydrogen bonds, highlighting the complex interplay between interactions and reaction outcomes in these nanostructured solvent systems.

Ionic liquids (ILs), low melting salts, have attracted increasing interest as solvents for chemical synthesis and for the extraction and valorisation of biomass, amongst other applications.[1-4] Much interest stems from the physicochemical properties of ILs, induced by the presence of strong Coulombic interactions between ions combined with weaker, directional interactions. These interactions lead to unique solution structures due to the presence of charge-ordering and the formation of amphiphilic nanostructures when ions containing alkyl chains of sufficient length are present as part of the IL, including in IL mixtures.[5-9] While the understanding of the effects of ion-solute interactions on reactivity has grown substantially over the past decade,[10-12] less is known about the potential role of the amphiphilic nanostructure of ILs on reactivity.[13, 14] The amphiphilic nanostructure of ILs has been shown to affect polymerisation reactions,[15, 16] Diels-Alder reactions[17] and selected nucleophilic substitution processes.[18, 19] The reactions affected by IL amphiphilic nanostructures tend to feature limited charge development from the initial state to the highest energy transition state in the reaction, meaning that structural effects do not compete with solvent reorganisation.[20, 21]

The homogeneous acid-catalysed dehydration (elimination) of alcohols does not feature substantial changes in the distribution of charge from the initial state to the highest energy transition state.[22] These reactions are of specific relevance for ILs given the importance of alcohol dehydration processes, particularly those of secondary alcohols, in the conversion of polysaccharides and sugars into platform chemicals such as 5-hydroxymethylfurfural (HMF).[23]

Kalviri et al. explored the dehydration of a range of secondary benzylic alcohols to alkenes using phosphonium ILs in conjunction with microwave heating.[24] This investigation identified that phosphonium ILs could facilitate the dehydration of alcohols without the addition of a separate acid catalyst, although the role of the IL amphiphilic nanostructure was not explored. Kumar et al. explored similar benzylic substrates for dehydration reactions performed within imidazolium ILs.[25] A screening process identified [C_6C_1im]Br (abbreviation from Figure 1) as the most effective IL for this reaction, surpassing [C_4C_1im]Br, which was attributed to the ease of extraction rather than a specific role of the amphiphilic nanostructure.

Towards determining whether the amphiphilic nanostructure of ILs affects the dehydration of secondary alcohols and to understand the origin of any effects, we initially explored the dehydration of cyclohexanol (CyOH) as a model substrate (Figure 1). CyOH was chosen as it does not lead to a complex product distribution and, unlike linear aliphatic secondary alcohols, cannot easily interdigitate with the IL alkyl chains.[19]

Reactions of CyOH were performed by heating a stirred solution of CyOH dissolved in the desired IL in a Teflon-lined hydrothermal reactor under autonomous pressure, with mesitylene added as an internal standard. The reaction was quenched in an ice bath, with exhaustive extraction of the IL phase by hexane followed by quantification of cyclohexene (Cyene) using GC-FID. As the aim was to assess changes in the reaction efficiency based on IL structural effects, no catalyst was used and reaction conditions were optimised to produce a quantifiable amount of Cyene, rather than to achieve the maximum Cyene yield, as this provided scope to assess the effect of IL structure on reactivity. The conditions selected involved heating for 3 h at 180°C with 25 wt% CyOH with respect to IL, as these reactions led to 25 ± 4% yield of Cyene in [$C_{10}C_1$im][NTf_2] (see ESI for details).

The yields of Cyene and conversions of CyOH observed under the standard reaction conditions are summarised in Table 1, alongside the mol% CyOH used in each reaction. It is apparent from that the Cyene yield was more reproducible than CyOH

[a] School of Chemical Sciences, The University of Auckland, Auckland, New Zealand. Email: cameron.weber@auckland.ac.nz
[b] MacDiarmid Institute for Advanced Materials and Nanotechnology, New Zealand.
[c] School of Science, Auckland University of Technology, Auckland, New Zealand.
Electronic Supplementary Information (ESI) available: detailed experimental procedures, further data and discussion. See DOI: 10.1039/x0xx00000x

Please do not adjust margins

conversion. This can be ascribed to the quantification method used, as the hexane extraction effectively separates Cyene but may leave residual CyOH in the IL phase. This accounts for the larger CyOH conversions observed compared to the Cyene yield in most cases. Small amounts of cyclohexanone were observed (< 3%, ESI), presumably from CyOH oxidation under the reaction conditions. The significant conversion of CyOH and low Cyene yield within $[C_{10}C_1im][Me_2PO_4]$ was likely due to a reaction between CyOH and the $[Me_2PO_4]^-$ anion. A new resonance was observed in the ^{31}P NMR of this reaction mixture, consistent with the formation of a phosphate ester (ESI). No reactions between CyOH and other ILs or general degradation of the ILs under the reaction conditions were observed.

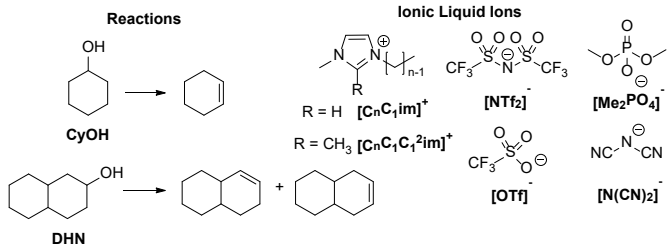

Fig. 1 Reactions studied and IL ions used in this work along with abbreviations used throughout.

Table 1. Initial mol% CyOH, Cyene yield and CyOH conversion within each IL solvent.[a] Reported errors are standard deviations obtained from replicate experiments.

IL	CyOH (mol%)	CyOH Conversion (%)	Cyene Yield (%)
$[C_2C_1im][NTf_2]$	45	59 ± 5	38.7 ± 0.1
$[C_4C_1im][NTf_2]$	48	58 ± 1	38.7 ± 0.1
$[C_6C_1im][NTf_2]$	47	52 ± 1	37.3 ± 0.1
$[C_8C_1im][NTf_2]$	50	38 ± 2	26.0 ± 0.1
$[C_{10}C_1im][NTf_2]$	51	43 ± 8	25 ± 4
$[C_4C_1im][OTf]$	32	0[b] (0[b])[c]	0.6 ± 0.1 (2.2 ± 0.3)[c]
$[C_{10}C_1im][OTf]$	42	14 ± 2 (10 ± 3)[c]	5 ± 2 (13 ± 2)[c]
$[C_4C_1im][N(CN)_2]$	30	0[b]	0.7 ± 0.1
$[C_{10}C_1im][Me_2PO_4]$	42	42 ± 6	0.3 ± 0.1

[a] Reaction performed at 180°C for 3 h with 20 wt% CyOH. [b] CyOH recovery > 100% observed. [c] Reaction performed for 18 h under the same conditions.

With respect to the trends observed for the ILs, it is clear that higher yields for the dehydration reaction were obtained in ILs containing the $[NTf_2]^-$ anion compared to ILs containing more strongly hydrogen-bond (H-bond) accepting anions such as $[N(CN)_2]^-$ or $[OTf]^-$. There is also an influence of the alkyl chain length of the IL cation, with $[C_nC_1im][NTf_2]$ ILs ($n \leq 6$) leading to improved Cyene yields compared to those where $n > 6$. The opposite is true of $[C_nC_1im][OTf]$ ILs where $n = 4$ leads to lower conversions and yields compared to $n = 10$. To ensure this wasn't an artifact caused by the low conversion, the reaction time was increased from 3 h to 18 h for the $[OTf]^-$ ILs which provided higher Cyene yields but the same trend.

Accounting for these trends requires insight into the underlying reaction mechanism. Given no acid catalyst has been added, the activation of the alcohol likely arises from protonation by the imidazolium cation, given the known acidity of these cations and their ability to form carbenes.[26] To test this proposal, $[C_4C_1C_1^2im][NTf_2]$ was explored as a solvent, as the methylation of the C2 position significantly reduces the Brønsted acidity of the imidazolium cation. No Cyene could be observed from the reaction of CyOH in this IL, compared to the 38.7% yield observed in $[C_4C_1im][NTf_2]$.

The mole fraction dependence of Cyene yield was studied in $[C_{10}C_1im][NTf_2]$ to examine the role of the IL concentration, which has been shown to influence reaction outcomes.[27] Figure 2 depicts the yield of Cyene against IL mole fraction. The maximum Cyene yield of 43% is reached at an IL mole fraction of 0.64. This highlights the potential role of IL as both a solvent and catalyst for this reaction, since diluting CyOH would be expected to decrease the rate of Cyene formation in the absence of specific solvent effects. Combined with the effect of $[C_4C_1C_1^2im][NTf_2]$, these results suggest the reaction proceeds via protonation of CyOH by the imidazolium cation, followed by a conventional E1 mechanism.[28]

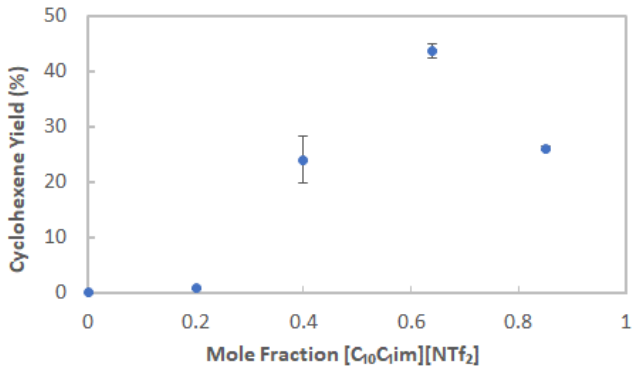

Fig. 2 Cyene yield dependence on $[C_{10}C_1im][NTf_2]$ mole fraction for reaction performed at 180°C for 3 h.

These results demonstrate two key effects influencing CyOH dehydration. The first is the anion effect whereby less basic anions (e.g. $[NTf_2]^-$) lead to more rapid dehydration than more basic anions such as $[OTf]^-$ and $[N(CN)_2]^-$. This can be rationalised by considering the effect of the IL anion on the acidity of the cation. Weakly interacting, less basic anions increase the acidity of the cation by reducing competition between the anion and CyOH for solvation by the cation.

The second effect relates to the influence of the alkyl chain. Increasing alkyl chain length leads to decreased Cyene for the $[NTf_2]^-$ ILs and an increased reaction rate in $[OTf]^-$ ILs. We have recently shown that CyOH resides predominantly in the polar domains of ILs that feature H-bond accepting anions whereas it is solvated to a greater extent in the non-polar domains of ILs featuring poor H-bond accepting anions.[29] Given the better H-bond accepting ability of the $[OTf]^-$ anion, this suggests the positive rate dependence on alkyl chain length may be caused by the increased concentration of CyOH in the polar domains within this IL; whereas the opposite effect in the $[NTf_2]^-$ IL implies reduced reactivity due to solvation in the non-polar domains, away from the catalytically active imidazolium cation. This highlights the potential influence of IL nanostructure in controlling the outcome of CyOH dehydration.

It was of interest to examine this further through a detailed kinetic analysis to obtain temperature dependent kinetic data

 This journal is © The Royal Society of Chemistry 20xx

Please do not adjust margins

Please do not adjust margins

and assess $\Delta^{\ddagger}H^{\ominus}$ and $\Delta^{\ddagger}S^{\ominus}$ for the reaction. Unfortunately, CyOH dehydration could not be studied under the reaction conditions due to the volatility of Cyene and low rate of reaction below 180°C. The substrate was changed to decahydro-2-naphthol (DHN) to yield less volatile reaction products but it was found that an acid catalyst (p-toluenesulfonic acid, p-TSA) was still required to provide a reaction rate sufficiently fast at a low enough temperature to facilitate kinetics experiments.

The dehydration of DHN was monitored by ^{1}H NMR with aliquots taken regularly from a stirred 0.65 M solution of DHN containing 20 mol% p-TSA and 1,3,5-trimethoxybenzene as an internal standard (see ESI for details). The reaction was first-order in DHN and the rate constants obtained in 4 ILs differing in alkyl chain length and anion are summarised in Table 2.

Table 2. Rate constants determined for the dehydration of DHN in ILs at different temperatures. Errors are standard errors obtained from replicate experiments.

T (°C)	$[C_4C_1im][NTf_2]$ (x 10^{-5} s^{-1})	$[C_{10}C_1im][NTf_2]$ (x 10^{-5} s^{-1})	$[C_4C_1im][OTf]$ (x 10^{-5} s^{-1})	$[C_{10}C_1im][OTf]$ (x 10^{-5} s^{-1})
100	2.2 ± 0.04	4.0 ± 0.2	1.4 ± 0.2	0.8 ± 0.06
105	4.5 ± 0.7	8.2 ± 2.4	3.7 ± 0.2	1.4 ± 0.06
110	8.8 ± 0.8	17.6 ± 0.5	5.7 ± 0.02	2.2 ± 0.1
115	16.2 ± 0.5	30.4 ± 2.9	10.9 ± 0.01	4.0 ± 0.06
120	27.4 ± 0.8	54 ± 2.9	17.9 ± 0.1	5.2 ± 0.4

For each temperature explored, DHN dehydration proceeded faster in $[NTf_2]$-based ILs. Elongation of the alkyl chain length from $[C_4C_1im]^+$ to $[C_{10}C_1im]^+$ led to rate enhancements for the $[NTf_2]^-$ ILs, whereas the opposite was observed for ILs containing the $[OTf]^-$ anion. This is the opposite trend to that observed for CyOH and suggests that the addition of p-TSA affects the reaction mechanism and hence the role of the IL.

To determine if the IL anion influenced the acidity of p-TSA, the Hammett acidity (H_0) of each solvent system was measured using the NMR method of Gräsvik et al.[30] The H_0 values of the $[C_4C_1im][NTf_2]$ and $[C_{10}C_1im][NTf_2]$ solutions were found to be similar with H_0 of −1.9 and −1.7 respectively, whilst the acidities of the $[OTf]^-$ ILs were below the minimum acidity detectable by the NMR probe used (Table S5). These results suggest that the origin of the improved reaction rates in $[NTf_2]^-$ ILs is due to the greater acidity of p-TSA in these systems relative to $[OTf]^-$ ILs. This does not account for the opposing trends upon elongation of the cation alkyl chain length.

Table 3 compiles the activation parameters derived from the Arrhenius and Eyring plots of the first-order rate constants (fitting details in ESI). These parameters are in general agreement with other reported secondary alcohol dehydration parameters.[28, 31] As shown by Table 3, the activation energy for both $[C_4C_1im][NTf_2]$ and $[C_{10}C_1im][NTf_2]$ were the same within uncertainty, whilst the pre-exponential factor was slightly larger for reactions performed within $[C_{10}C_1im][NTf_2]$. For the $[OTf]^-$ ILs, increasing the alkyl chain length of the cation led to a reduction in activation energy accompanied by a large decrease in the pre-exponential factor.

$\Delta^{\ddagger}H^{\ominus}$ values for both $[NTf_2]^-$ ILs were within experimental error; however, $\Delta^{\ddagger}S^{\ominus}$ differs, with $\Delta^{\ddagger}S^{\ominus}$ being more favourable within $[C_{10}C_1im][NTf_2]$, in accordance with the higher rate constants observed in this IL. The higher $\Delta^{\ddagger}S^{\ominus}$ for $[C_{10}C_1im][NTf_2]$ may be a result of reduced ordering around the transition state or increased organisation about the starting materials. The latter seems more likely, and may reflect the organisation associated with solvation of DHN near the polar/non-polar domain interface in the larger non-polar domains of $[C_{10}C_1im][NTf_2]$ compared to $[C_4C_1im][NTf_2]$ where the smaller domain size would preclude the solvation of DHN solely within the non-polar domain. In contrast, dramatic changes in activation parameters were observed for the $[OTf]^-$ ILs, with both $\Delta^{\ddagger}H^{\ominus}$ and $\Delta^{\ddagger}S^{\ominus}$ significantly lower for reactions performed in $[C_{10}C_1im][OTf]$ compared to $[C_4C_1im][OTf]$ or the $[NTf_2]^-$ ILs. This indicates that DHN dehydration is more enthalpically favourable within $[C_{10}C_1im][OTf]$ compared to the other ILs but this is offset by being substantially less entropically favourable.

Table 3. Arrhenius and Eyring parameters determined for the dehydration of DHN in ILs. Errors are standard errors obtained from the linear fits.

Ionic liquid	E_a (kJ mol^{-1})	A (x 10^{14} s^{-1})	$\Delta^{\ddagger}H^{\ominus}$ (kJ mol^{-1})	$\Delta^{\ddagger}S^{\ominus}$ (J K^{-1} mol^{-1})
$[C_4C_1im][NTf_2]$	155 ± 4	1200 ± 40	152 ± 4	73 ± 3
$[C_{10}C_1im][NTf_2]$	159 ± 8	7300 ± 500	156 ± 5	88 ± 4
$[C_4C_1im][OTf]$	150 ± 10	180 ± 20	148 ± 10	57 ± 6
$[C_{10}C_1im][OTf]$	120 ± 7	0.0049 ± 0.0004	117 ± 7	-31 ± 3

The most probable explanation for these observed trends in activation parameters is the existence of a pre-organised H-bond cluster between DHN and p-TSA within the non-polar domains of $[C_{10}C_1im][OTf]$. Non-polar environments tend to promote H-bonding between non-ionised compounds, since the formation of ions is unfavourable.[32] Therefore, instead of a formal acid-base reaction occurring, an initial formation of an alcohol-acid 'dimer' may occur based on a H-bond between p-TSA and DHN (Scheme 1). This would make the mechanism more enthalpically favourable, reducing the energy required to formally protonate the alcohol, but less entropically favourable due to the association of reactants. The reaction would then proceed by proton transfer from the H-bond dimer to form an oxonium intermediate prior to loss of water which is likely to occur through an E1 mechanism.[28] Since the H-bond cluster is presumed to reside within the non-polar domains where there is less competition from IL ions, a significant amount of reorganisation would be needed upon formation of the charged transition state, hence the lower pre-exponential factor and negative $\Delta^{\ddagger}S^{\ominus}$.[20, 21]

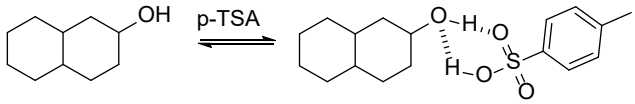

Scheme 1. The formation of the putative acid-alcohol H-bond dimer between DHN and p-TSA.

While this explanation would account for the activation parameters observed in $[C_{10}C_1im][OTf]$, it remains to explain why this differs from the other ILs. Due to the presence of a smaller, more strongly interacting anion, $[C_{10}C_1im][OTf]$ possesses more pronounced polar and non-polar domains than $[C_{10}C_1im][NTf_2]$.[33] It is likely that this increased nanostructural segregation in $[C_{10}C_1im][OTf]$ leads to greater

Please do not adjust margins

Please do not adjust margins

compartmentalisation of DHN and p-TSA within either the polar or non-polar domains. Due to the stronger H-bond accepting ability and increased basicity of the $[OTf]^-$ anion compared to the $[NTf_2]^-$ anion, less 'free' p-TSA and DHN would be present within the polar domains due to their more favourable interaction with the ions, leading to the initiation of a reaction pathway within the non-polar rather than polar domains.

The similarity in activation parameters observed for the $[NTf_2]^-$ ILs can be rationalised by the strength of interion interactions. Due to the weaker interactions between $[C_{10}C_1im]^+$ and $[NTf_2]^-$, the nanostructured domains formed are less well-defined than in the corresponding $[OTf]^-$ system. The larger interion distances may result in reduced partitioning of the acid and alcohol within the non-polar domains of $[C_{10}C_1im][NTf_2]$. Also, the reduced influence of DHN-ion and acid-ion interactions increases the importance of interactions between DHN and acid within the polar domains of these ILs, reflected in the reduced influence of nanostructure on reaction outcomes.

In summary, we have shown that the amphiphilic nanostructures of ILs can have notable effects on alcohol dehydration processes. Rather than a general effect, the influence of the nanostructure depends on the nature of the reaction mechanism and specific solvent-solute interactions. Understanding and manipulating these interactions may create opportunities to perform important alcohol dehydration processes, including biomass transformations, at similar rates but at much lower temperatures than are currently used. This is foreshadowed by the notable increase in $\Delta^{\ddagger}S^{\ominus}$ for DHN dehydration in $[C_{10}C_1im][OTf]$ relative to other ILs. Investigations of more complex alcohol dehydration processes are currently underway in our laboratory to fully elucidate these nanostructure effects.

This work was funded by a Science for Technological Innovation National Science Challenge seed grant, UOAX1906.

Conflicts of Interest

There are no conflicts to declare.

Notes and references

1. J. P. Hallett and T. Welton, *Chem. Rev.*, 2011, **111**, 3508-3576.
2. A. Brandt, J. Gräsvik, J. P. Hallett and T. Welton, *Green Chem.*, 2013, **15**, 550-583.
3. J. B. Harper and M. N. Kobrak, *Mini-Rev. Org. Chem.*, 2006, **3**, 253-269.
4. R. Prado and C. C. Weber, in *Application, Purification and Recovery of Ionic Liquids*, eds. O. Kuzmina and J. P. Hallett, Elsevier B. V., Amsterdam, Netherlands, 2016, ch. 1, pp. 1-58.
5. R. Hayes, G. G. Warr and R. Atkin, *Chem. Rev.*, 2015, **115**, 6357-6426.
6. Y. Wang and G. A. Voth, *J. Am. Chem. Soc.*, 2005, **127**, 12192-12193.
7. O. Russina, A. Triolo, L. Gontrani and R. Caminiti, *J. Phys. Chem. Lett.*, 2012, **3**, 27-33.
8. C. P. Cabry, L. D'Andrea, N. S. Elstone, S. Kirchhecker, A. Riccobono, I. Khazal, P. Li, S. E. Rogers, D. W. Bruce and J. M. Slattery, *Phys. Chem. Chem. Phys.*, 2022, **24**, 15811-15823.
9. O. Hollóczki, M. Macchiagodena, H. Weber, M. Thomas, M. Brehm, A. Stark, O. Russina, A. Triolo and B. Kirchner, *ChemPhysChem*, 2015, **16**, 3325-3333.
10. S. T. Keaveney, R. S. Haines and J. B. Harper, *Pure Appl. Chem.*, 2017, **89**, 745-757.
11. A. Schindl, R. R. Hawker, K. S. Schaffarczyk McHale, K. T. C. Liu, D. C. Morris, A. Y. Hsieh, A. Gilbert, S. W. Prescott, R. S. Haines, A. K. Croft, J. B. Harper and C. M. Jäger, *Phys. Chem. Chem. Phys.*, 2020, **22**, 23009-23018.
12. J. P. Hallett, C. L. Liotta, G. Ranieri and T. Welton, *J. Org. Chem.*, 2009, **74**, 1864-1868.
13. J. C. S. Terra, A. R. Martins, F. C. C. Moura, C. C. Weber and A. Moores, *Green Chem.*, 2022, **24**, 1404-1438.
14. N. K. Kahlon and C. C. Weber, *Aust. J. Chem.*, 2022, **75**, 9-23.
15. S. Puttick, A. L. Davis, K. Butler, D. J. Irvine, P. Licence and K. J. Thurecht, *Polym. Chem.*, 2013, **4**, 1337-1344.
16. S. Puttick, A. L. Davis, K. Butler, L. Lambert, J. El harfi, D. J. Irvine, A. K. Whittaker, K. J. Thurecht and P. Licence, *Chem. Sci.*, 2011, **2**, 1810-1816.
17. D. W. Bruce, Y. Gao, J. N. Canongia Lopes, K. Shimizu and J. M. Slattery, *Chem. Eur. J.*, 2016, **22**, 16113-16123.
18. C. C. Weber, A. F. Masters and T. Maschmeyer, *Angew. Chem. Int. Ed.*, 2012, **51**, 11483-11486.
19. C. C. Weber, A. F. Masters and T. Maschmeyer, *Org. Biomol. Chem.*, 2013, **11**, 2534-2542.
20. H. M. Yau, S. A. Barnes, J. M. Hook, T. G. A. Youngs, A. K. Croft and J. B. Harper, *Chem. Commun.*, 2008, 3576-3578.
21. H. M. Yau, A. G. Howe, J. M. Hook, A. K. Croft and J. B. Harper, *Org. Biomol. Chem.*, 2009, **7**, 3572-3575.
22. P. Kostetskyy, N. A. Zervoudis and G. Mpourmpakis, *Catal. Sci. Technol.*, 2017, **7**, 2001-2011.
23. C. G. Yoo, Y. Pu and A. J. Ragauskas, *Curr. Opin. Green Sustain. Chem.*, 2017, **5**, 5-11.
24. H. A. Kalviri and F. M. Kerton, *Adv. Synth. Catal.*, 2011, **353**, 3178-3186.
25. R. Kumar, A. Sharma, N. Sharma, V. Kumar and A. K. Sinha, *Eur. J. Org. Chem.*, 2008, **2008**, 5577-5582.
26. N. M. A. N. Daud, E. Bakis, J. P. Hallett, C. C. Weber and T. Welton, *Chem. Commun.*, 2017, **53**, 11154-11156.
27. A. Gilbert, R. S. Haines and J. B. Harper, *Org. Biomol. Chem.*, 2019, **17**, 675-682.
28. Y. Liu, A. Vjunov, H. Shi, S. Eckstein, D. M. Camaioni, D. Mei, E. Baráth and J. A. Lercher, *Nat. Commun.*, 2017, **8**, 14113.
29. D. Yalcin, I. D. Welsh, E. L. Matthewman, S. P. Jun, M. McKeever-Willis, I. Gritcan, T. L. Greaves and C. C. Weber, *Phys. Chem. Chem. Phys.*, 2020, **22**, 11593-11608.
30. J. Gräsvik, J. P. Hallett, T. Q. To and T. Welton, *Chem. Commun.*, 2014, **50**, 7258-7261.
31. F. Chen, M. Shetty, M. Wang, H. Shi, Y. Liu, D. M. Camaioni, O. Y. Gutiérrez and J. A. Lercher, *ACS Catal.*, 2021, **11**, 2879-2888.
32. M. M. Davis, *Acid-base behavior in aprotic organic solvents*, US National Bureau of Standards, 1968.
33. A. M. Fernandes, M. A. A. Rocha, M. G. Freire, I. M. Marrucho, J. A. P. Coutinho and L. M. N. B. F. Santos, *J. Phys. Chem. B*, 2011, **115**, 4033-4041.

This journal is © The Royal Society of Chemistry 20xx

Please do not adjust margins